

Identification of Time-Variant Directional Mobile Radio Channels

R.S. Thomä, D. Hampicke, A. Richter, G. Sommerkorn, A. Schneider, U. Trautwein

Department of Electrical Engineering and Information Technology

Ilmenau University of Technology

P.O.B. 100565, D-98684 Ilmenau, Germany

Phone: (+49) 3677-692622, Fax: (+49) 3677-691113, E-mail: tho@e-technik.tu-ilmenau.de

<http://www-emt.tu-ilmenau.de>

Abstract

For the real-time identification of the time-variant, directional structure of the mobile radio channel impulse response, a broadband vector channel sounder is described. The measurement procedure relies on periodic multi-frequency excitation signals, correlation processing and joint delay-azimuth superresolution based on the ESPRIT algorithm. The underlying signal model is developed and the different possibilities of ESPRIT application are discussed. Problems of imperfect receiver and antenna performance and the appearing resolution limits are outlined. Results of multidimensional correlation analysis of various channel scenarios in the Doppler-delay-angular domain are presented.

1 Motivation

Efficient wireless transmission constitutes a key technology for future universal mobile communication systems. High data rates, adequately defined quality of service, high system capacity and high bandwidth efficiency require new and sophisticated radio link designs. That includes adaptive equalization and adaptive modulation schemes. Most recently, smart antenna principles are considered to enhance system performance. The expected benefits include increased capacity and quality of service as a result of interference reduction by spatial filtering and sophisticated equalization and diversity procedures in the joint delay and angular domain [1].

Design and simulation of smart antenna modems requires profound knowledge of the radio channel impulse response (CIR) statistics [2]. The multipath components of the time-variant impulse response have to be analyzed with respect to their path delays and directions of arrival. Wideband, real-time measurement of the time-variant directional radio channel is a very demanding task. High multipath time delay and angular resolution as well as fast measurement repetition rate are required. Traditional measurement methods based on swept network analyzers or sliding correlators and rotating antennas are generally not suited since they presume time-invariant radio channels.

The paper describes the basic performance of the antenna array based Vector Radio Channel Sounder RUSK ATM. The parametric signal model and the estimation procedure are outlined. Finally, an introduction to the statistical analysis of the channel characteristics and some measured examples are given. The channel sounder has been developed under the german national project line ATMmobil which is designated for next generation broadband multimedia mobile radio systems.

2 Signal model

The signal transmission in a typical mobile radio channel is affected by time-angular-variant multipath propagation as indicated in Fig. 1. In the uplink the waves impinging on the base station (BS) antenna consist of a line-of-sight component (LOS) and contributions from $K-1$ non-LOS paths with relative ex-

cess delays from different directions that result from scattering, reflection or diffraction. The individual path contributions are time-varying because of mobile station (MS) and environmental objects movement. Generally, the path weights $\gamma_k(t)$ may be fast fading since in some microscopic sense (not resolved by the respective measurement resolution in time and/or azimuth) any scattered and diffracted path consists of a superposition of time-variant contributions. Therefore, for some limited observation time, the channel impulse response is often considered as a wide-sense stationary stochastic process (WSS). For a longer observation time and MS traveling distances of much more than (typically) some tens of the carrier wavelengths, the mean path time-delays τ_k (TDOA), the directions of arrival θ'_k (DOA), the Doppler shifts α_k and the dominant path numbers K are varying and the r.m.s. path weights become slowly fading because of the changing scenario geometry and possible path shadowing and varying path loss. Thus, the time-space-variant impulse response can be given as:

$$h_{t,s}(t, \tau, s) = \sum_{k=1}^K \gamma_k(t) e^{-j2\pi t \alpha_k} e^{-j2\pi s \theta_k} \delta(\tau - \tau_k) \quad (1)$$

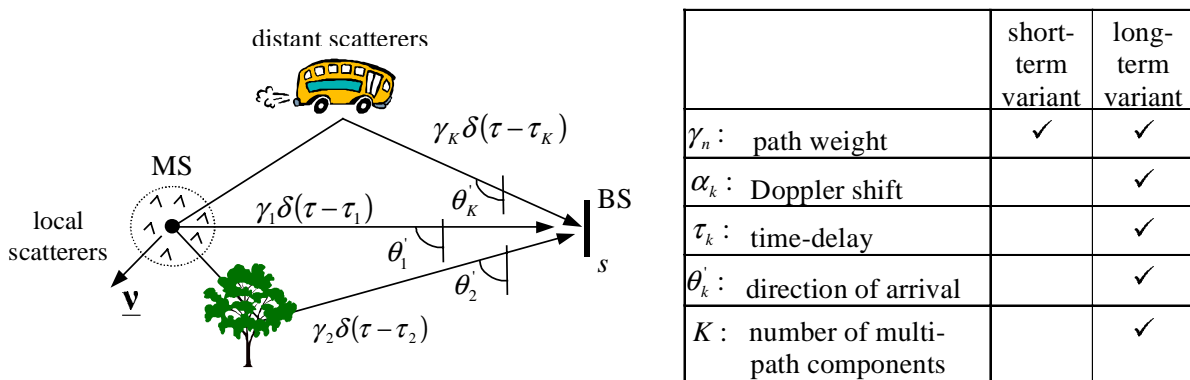


Fig. 1: Time-angular-variant multipath propagation in a mobile radio link.

The channel response in (1) represents the channel in the equivalent baseband domain. The parameters have to be considered as valid in some limited frequency range only. Since we restrict our discussion to azimuthal DOA, the space domain variable s is appropriately defined by the linear BS antenna aperture. We also assume plane wavefronts. E.g., for object distances $r > 28.5 S\lambda_0$ we get up to $\pm 0.5^\circ$ phase error along the aperture [3]. Furthermore, the wavefront delays along s can be approximated by the complex phasor multiplication $\exp(-j2\pi s \theta_k)$ if the signals are narrowband and the antenna aperture is small enough, $S\lambda_0 \ll c/B$. Here c is the velocity of light, B is the measurement bandwidth and S is the maximum antenna aperture. Both, s and S are given normalized to the wavelength λ_0 at the carrier frequency. The projection of the waves from azimuthal DOAs θ' to the antenna aperture results in the directional cosines $\theta_k = \cos(\theta'_k)$.

The parametric linear input/output signal model from (1) is more clearly arranged if we use the appropriate Fourier transform relations

$$\begin{aligned} \alpha, \tau, \theta & \circlearrowleft & h(\alpha, \tau, \theta) &= \sum_{k=1}^K \Gamma_k(\alpha) * \delta(\alpha - \alpha_k) \delta(\tau - \tau_k) \delta(\theta - \theta_k) \\ t, f, s & \bullet & H(t, f, s) &= \sum_{k=1}^K \gamma_k(t) e^{-j2\pi t \alpha_k} e^{-j2\pi f \tau_k} e^{-j2\pi s \theta_k} \end{aligned} \quad (2)$$

The Doppler-azimuth-variant impulse response is related to the time-space-variant frequency response by a 3-D Fourier transform. Note, that it is the linear array assumption that results in a Fourier transform relation for the space-azimuth branch of the transform. The time-Doppler Fourier pair shows that fast

fading path weights $\chi_k(t)$ introduce local Doppler spread. If single reflections are resolved, that results in pure Doppler shift and constant path weight magnitudes. Only then the channel parameter estimation procedure may be considered as a three-dimensional harmonic retrieval problem.

3 Vector radio channel sounder hardware design

Depending on the available hardware, the measurement of the system response functions in (2) can be performed in any domain of the transform pairs. By all means, the resolution of the parameter triple $\alpha_k, \tau_k, \theta_k$ is given by the resulting aperture sizes T, B, S in the t, f, s -domain which are limited by the signal model restrictions and the hardware constraints. The latter are imposed by the instantaneous bandwidth B from ADC/DAC sampling rate limitations and by the antenna aperture from receiver channel number limitations. At the same time the narrow band modeling assumption required to establish (1) imposes constraints on the bandwidth and the antenna aperture. The maximum measurement time aperture T is limited by the invariance condition of the channel parameters. On the other hand, the measurement repetition rate has to be fast enough in order to reproduce the time variation by meeting the Nyquist sampling criterion w.r.t. variable t which is given by the expected maximum Doppler bandwidth. Therefore, the hardware design for a real-time vector channel sounder is a demanding task that requires very fast processing. The remaining margin for measurement time stretching by cost saving sequential operations is given by the delay-Doppler spread factor, which is defined by the product of the maximum excess delay and the maximum Doppler bandwidth. For a typical mobile radio channel, as a result of the path loss and the specified maximum transmit power and because of the maximum Doppler bandwidth, it is well below 1 %. In the terminology of time-variant linear systems [4], the mobile radio channel is clearly "underspread". Since the vector channel sounder RUSK ATM relies on real-time sampling instead of sliding correlation, sequential operation in the spatial domain can still be used without sacrificing the advantage of having full real-time access to the time-variant radio channel. By fast antenna multiplexing, the individual antenna responses that form the channel response vector snapshot (CRVS) are sequentially estimated. The multiplexer timing is synchronized to consecutive periods of the Tx signal. Since only a single RF downconverter channel is required, the hardware expense is reduced dramatically as compared to a completely parallel multichannel operation. Details of the hardware design are described in [6]. Table 1 gives an overview of the resulting hardware parameters.

Instantaneous bandwidth	120 MHz		
Frequency range	5 ... 6 GHz (extension available)		
Scalar impulse response	Response length: 0.8 ... 25.6 μ s Dynamic range: 35 dB		
Antenna array	8 elements, multiplexed		
Measurement mode	Event triggered	Standard Doppler	Fast Doppler
Repetition rate	50 Hz	1 kHz	\approx 70 kHz
Time record length (8 channels, 0.8 μ s impulse response)	limited by external DAT capacity	\approx 60 s	256 snapshots
Tx/Rx sync	Rubidium reference / optical fiber		
Interfaces	DAT streamer, SCSI, TFT-Display, telemetry, GPS / DGPS, odometer and gyrosscopic sensor interface		

Table 1: Basic hardware parameters of RUSK ATM vector channel sounder.

The measurement setup consists of a mobile transmitter (Tx) that acts as the MS and of a fixed receiver (Rx) that plays the role of the BS. 120 MHz bandwidth periodic multi-frequency excitation signals with

minimum crest factor are used. Those signals are very effective for frequency domain system identification since they offer an exactly limited frequency spectrum, allow fast measurements and low estimation variance as well as minimum leakage bias in case of synchronized FFT processing [5]. The signal is generated in the RF-range by upconversion from the baseband and radiated with a power of 26 dBm from an omnidirectional monopole antenna. The 5.2 GHz Rx antenna is formed by an $M=8$ element uniform linear array (ULA) of $\lambda_0/2$ spaced planar elements, which are vertically polarized and have 120° azimuthal beamwidth. The choice of the antenna array geometry strongly influences the DOA estimation performance. As will be seen later, a ULA geometry allows very effective algorithms from a computationally point of view. For any array output $m = 1 \dots M$, the receive signal spectrum $\hat{Y}(n, \mu, m)$ is calculated by FFT and an estimate of the CRVS in the frequency domain is calculated as $\hat{H}(n, \mu, m) = \hat{Y}(n, \mu, m) / \hat{X}(n, \mu, m)$ with the argument variables n, μ denoting the snapshot time instant nt_0 and the frequency $\mu f_0 = \mu / t_p$, resp. The excitation signal reference spectrum $\hat{X}(n, \mu, m)$ is measured by a back-to-back calibration procedure where the radio channel is replaced by an attenuator connected between Tx and Rx. Therefore, Tx- and Rx-frequency response and nonlinear distortion of the Tx power amplifier are removed from the measurement results [13].

4 Channel parameter estimation

For evaluation of micro- and especially of picocell-scenarios, very high path parameter resolution is required. Even if aperture sizes in the three domains are chosen as large as possible, simple DFT estimation of the discrete parameters in (2) would not yield satisfactory results. Firstly, angular resolution is limited by the array aperture to $0.89/S$ which corresponds to about 12.5° of DOA resolution in case of the $S = 4$ array at broadside direction. It even reduces to about 30° at the skirts of the beam sector. Secondly, the τ_k resolution in the delay domain is in the order of 8 to 15 ns which corresponds to 2.4 to 4.5 m, depending upon the window function in the frequency domain that is used for CIR sidelobe reduction. Even Doppler resolution can be a problem when the time aperture length is strongly limited, especially for rapidly changing scenarios. To overcome the DFT resolution limits, parametric DOA estimation is applied in order to achieve superresolution. From the different procedures [8], the ESPRIT-type algorithms are especially suited for ULAs. As compared to other algorithms, such as Maximum Likelihood (see e.g. [9] for an effective iterative implementation for channel sounder application), the ESPRIT algorithm (Estimation of Signal Parameters via Rotational Invariance Techniques) is very time-effective since it avoids extensive multidimensional search. The matrix model for estimation is given as:

$$\mathbf{H}(n, \mu) = \mathbf{A}(\theta) \mathbf{\Gamma}(n, \mu) + \mathbf{N}(n, \mu) \quad (3)$$

with the frequency domain CRVS vector $\mathbf{H}(n, \mu) = [\hat{H}(n, \mu, 1) \dots \hat{H}(n, \mu, M)]$, the spatially white noise vector $\mathbf{N}(n, \mu)$ and the impinging wavefront vector $\mathbf{\Gamma}(n, \mu) = [\gamma_1 \exp(-j2\pi\mu f_0 \tau_1) \dots \gamma_K \exp(-j2\pi\mu f_0 \tau_K)]^T$. The $M \times K$ array response matrix $\mathbf{A}(\theta)$ is composed of the response vectors for the K individual wavefronts $\mathbf{a}(\theta_k) = [1, \exp(-j2\pi d \theta_k) \dots \exp(-j2\pi(M-1)d \theta_k)]^T$ where d gives the distance between the antennas normalized to the wavelength λ_0 . (3) represents the discrete, measured representation of the signal model (2) in the t, f, s -domain. Since the parametric approach can be considered as an alternative to the DFT, there are several possibilities to use superresolution algorithms for estimating the model parameters $\tau_k, \theta_k, \alpha_k$. E.g., only a single Fourier transform branch can be replaced by a 1-dimensional ESPRIT estimation. Since the most severe resolution restriction seems to be imposed by the antenna aperture, we start with the space (s) to azimuth (θ) transform. Fig. 2 gives an idea of the resulting procedure. With respect to the estimation of the remaining parameters τ_k, α_k the DFT-approach is used. In order to simplify the presentation, only the

delay-azimuth estimation is shown and the time-Doppler domain is omitted. The first step is to transform the frequency domain CRVS to the delay domain by DFT. Then a 1-D ESPRIT DOA estimation is applied for all τ_k bins that contain enough energy. This explains how high measurement bandwidth supports resolution of a large number of paths since only those paths that show the same path delay (within the delay resolution limit) have to be resolved in the azimuthal domain. The picture, however, also explains that the τ_k, θ_k estimation task can more consequently be characterized as a 2-D joint delay-angular estimation problem.

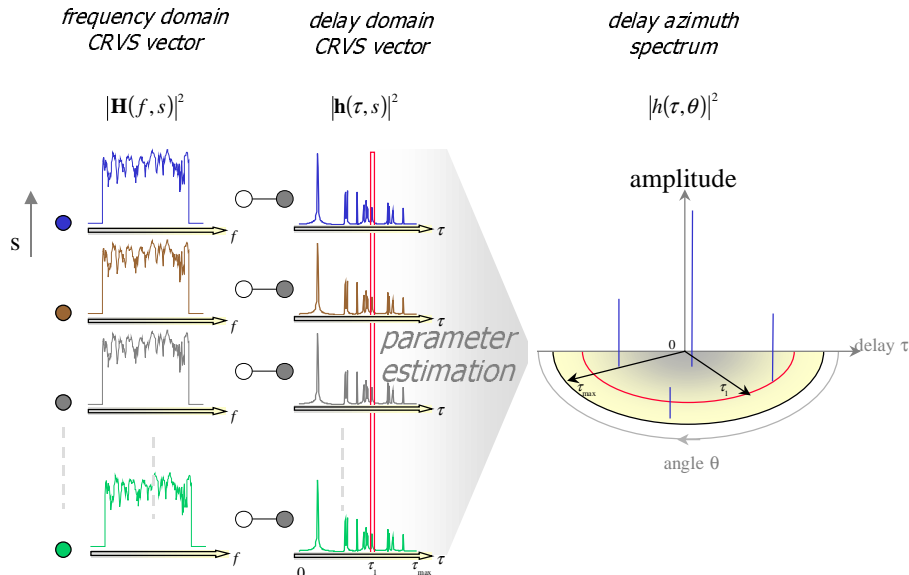


Fig. 2: Delay-azimuth snapshot estimation from one frequency domain CRVS.

Like other DOA estimation algorithms, the ESPRIT belongs to the subspace class that exploits the eigenvector structure of the array covariance matrix in order to estimate the signal subspace. Its efficiency, however, comes from the usage of the special structure of the array response matrix. In case of an ULA, $\mathbf{A}(\theta)$ takes the form of a Vandermonde matrix. The main idea of the ESPRIT is to divide it into two submatrices that correspond to identical sub-arrays which may even be arranged partly overlapping in space. Then there exists a projection matrix that uniquely rotates the output of one sub-array to the other. The actual estimation problem is now reduced to find that projection matrix by solving a general least-squares problem (LS-ESPRIT) of the resulting (typically) overdetermined set of equations. The eigenvalues of that projection matrix are directly related to the DOAs. Estimation accuracy can be enhanced by using structured or total least squares (SLS-ESPRIT, TLS-ESPRIT). The standard ESPRIT approach is even outperformed by the recently introduced unitary ESPRIT algorithm [10], [11]. That procedure transforms the subspace estimation step to a real problem by exploiting the structure of centro-symmetric arrays (as it is given by an ULA). Thereby, the estimated twiddle factors are constraint to the unit circle which reduces estimation errors. Moreover, unitary ESPRIT may be arranged to inherently contain forward-backward averaging. A further advantage of that idea is that it can be extended to a closed form 2-D joint parameter estimation algorithm that provides automatically paired sets of parameters. That allows a very smart solution of the joint delay-azimuth estimation problem described by Fig. 2 and (2) whereby also the delay resolution is enhanced by the superresolution capability of the ESPRIT. For more details see [3], [11].

As a result of the underlying stochastic model, proper estimation of the signal subspace is an issue. Since the CRVS (2) is assumed to be WSS with uncorrelated path scattering processes $\mathcal{Y}_k(t)$ some time

domain averaging is required in order to get a stable estimate. The maximum allowable time interval for averaging is given by the invariance condition of the slowly varying model parameters (s. Fig.1). Alternatively to the covariance averaging approach, there exists the direct data approach that uses singular value decomposition (SVD) of the same time sequence interval of the CRVS. That is often preferred because of a better numerical stability. Finally, the ESPRIT ends with an estimate of one set of the mean channel parameters τ_k, θ_k for the time interval considered. Then it is still necessary to estimate the path weights $\gamma_k(t)$. Since they are generally fast fading, they have to be determined consecutively for any single snapshot in time by least squares estimation of K sets of nullsteering beamformer weights using a Penrose-Moore pseudoinverse. The result is a sequence of snapshots in time that directly corresponds to the time-azimuth-variant impulse response $h_r(t, \tau, \theta)$. A Fourier transform w.r.t. time t results in the Doppler-azimuth-variant impulse response of (2).

Unfortunately, the azimuthal signal subspace decomposition fails if impinging wavefront signals are correlated. Since all paths are launched from the same source, reflected signals have to be considered as coherent if they are subjected to nearly the same delay (within the time resolution limits) and if the related scattering process is at least partly deterministic. In particular, the ability to resolve closely spaced paths is reduced dramatically [8]. Then spatial smoothing of the estimated signals subspace has to be performed for a rank enhancement. Since for that purpose the array has to be divided into overlapping subarrays to be smoothed, the effective array aperture is reduced. Thus, the maximum number of sources that can be resolved by the $M=8$ ULA at any delay bin is reduced to about 5. In case of joint delay-azimuth estimation also frequency domain smoothing is required in order to enhance delay subspace separation of paths from (nearly) the same azimuthal DOA. Of course, subspace smoothing not only enhances the rank of the signal subspace, it also improves statistical stability by noise reduction.

The quality of the whole procedure is also strongly influenced by the correct choice of the model order, but that cannot be discussed here.

5 Measurement Errors, Calibration and Resolution

In any practical measurement setup the acquired data are somewhat impaired by limited accuracy, noise and interference. Since a superresolution procedure can be understood as an extrapolation in the corresponding aperture domain, it is very sensitive to measurement errors. Therefore, the achievable resolution is limited by noise and device parameter impairments. As a general rule, amplitude and phase uniformity of the array channels determines the achievable DOA resolution while frequency domain invariability determines the TDOA resolution.

Since the RUSK ATM receiver consists only of a single down-converter channel, there are strongly reduced problems with unequal receiver channels. Mainly phase noise of the mixer frequency sources is an issue since the antenna outputs are sampled sequentially in time. In the device described phase noise is kept low enough by sophisticated PLL/VCO design. Antenna impairments, however, cause more problems. Because of the close spacing between neighboring elements, parasitic electromagnetic coupling cannot be avoided. That results in severe distortions of the antenna beam patterns. Although ESPRIT does not require the precise knowledge of the array response vector, it relies on identical beam patterns. Any non-uniformity of the beams disturbs the ESPRIT since the algorithm interprets that distortion as a result of impinging waves. Simulation has shown that the maximum peak-to-peak ripple of the resulting beam patterns should be below 0.5 dB in order to achieve 5° angular resolution of coherent paths. That can only be reached with sophisticated antenna array calibration. The calibration procedure is based on a set of reference measurements using a single source under well-defined propagation conditions in an anechoic

chamber with constant delay τ_k at an equidistant grid of well known azimuth angles θ_k . Details of an effective eigenvector-based calibration matrix estimation procedure and measured results are given in [12]. Stable 5° resolution of two sources impinging with the same TDOA has been demonstrated over the complete 120° azimuthal antenna sector with some degradation only at the skirts of the beams. Also the most complicated 5 coherent source scenario can be resolved [6]. It has been shown that parasitic echoes during calibration have to be at least 30 dB down if they are not clearly resolved in delay. Otherwise the calibration result is severely impaired.

Imperfect frequency response uniformity of the calibrated device results from remaining internal reflections that may be introduced by mismatch between the calibration and the measurement setup and from slightly changing frequency response as a result of AGC switching. Currently, about 1.5 ns TDOA resolution of sources impinging from the same DOA is reliably achieved which corresponds to about 50 cm spatial resolution.

6 Second Order Statistical Analysis

Because of the underlying stochastic signal model, statistical analysis based on second order correlation can reveal interesting channel features. The WSSUS channel model helps to define a 3-dimensional correlation function by assuming stationarity w.r.t. time, frequency and spatial distance ($\Delta t, \Delta f, \Delta s$). That corresponds to uncorrelated behavior w.r.t. the variables Doppler shift, delay and azimuth (α, τ, θ). The following 3D-Fourier-Transform relates the expected Doppler-delay-azimuth spectrum to the corresponding expected time-frequency-spatial correlation:

$$\begin{aligned} \alpha, \tau, \theta \circ \quad r(\alpha, \tau, \theta) &= \mathbb{E}\{|h(\alpha, \tau, \theta)|^2\} \\ \Delta t, \Delta f, \Delta s \bullet \quad R(\Delta t, \Delta f, \Delta s) &= \mathbb{E}\{H(t, f, s) H^*(t + \Delta t, f + \Delta f, s + \Delta s)\} \end{aligned} \quad (4)$$

The estimation of (5) should be based on the spectral domain α, τ, θ since that avoids time-expensive correlogram calculation. From classical spectral estimation of stochastic processes [14] it is well-known that some statistical averaging or smoothing is required in order get stable estimates. The relative variance of the estimation is inversely proportional to some aperture-resolution product. That means, there is a tradeoff of statistical stability against resolution that further aggravates the resolution constraints. From a computational point of view, one possibility is to smooth the rough estimate of the magnitude squared Doppler-azimuth variant impulse response by the smoothing window $W(\cdot)$:

$$\hat{r}(\alpha, \tau, \theta) = \iiint W(\alpha - \alpha', \tau - \tau', \theta - \theta') |h_{TBS}(\alpha', \tau', \theta')|^2 d\alpha' d\tau' d\theta' \quad (5)$$

The index in h_{TBS} denotes a *TBS* aperture limited estimate of the Doppler-azimuth variant impulse response (2). The smoothing impact of $W(\cdot)$ is determined by its spread in the different domains which shows the compromise between variance reduction and resolution bias. Therefore, the support of $W(\cdot)$ in each of the different domains has to be chosen deliberately in order to match the desired resolution of the path clusters. If the channel has to be evaluated from the viewpoint of some prospective application system, one objective may be to meet the resolution limits of that system. Another estimation possibility is to divide the time sequence $h_i(t, \tau, \theta)$ with the total aperture record length T into smaller, weighted and overlapping segments and proceed with spectral averaging. In that case, Doppler and delay resolution have to be chosen in advance, but eventually both procedures can be effectively combined [14].

As discussed in section 5, the maximum achievable delay-azimuth resolution corresponds to scattering clusters of about 50 cm in diameter. Therefore, with the carrier frequency of 5.2 GHz, only about

10 Doppler cycles are available. In that case it seems not appropriate to stake on DFT Doppler resolution. Then some parametric spectral resolution procedure should be applied to achieve reliable, high resolution estimates from the short time segments. Standard AR estimators seem to be well suited since at the same time a parametric channel model arises that is well suited for statistical channel modeling [17].

The general WSSUS relation (4) offers a large variety of deduced functions by applying Fourier transform relations w.r.t. the different variables as given in Fig 3. Reduced domain functions and parameters are calculated by integration over one, two or three variables such as the Doppler-delay spectrum, the delay-azimuth spectrum, the Doppler-azimuth spectrum, the delay spectrum or the Doppler spectrum, the Doppler spread or angular spread etc.

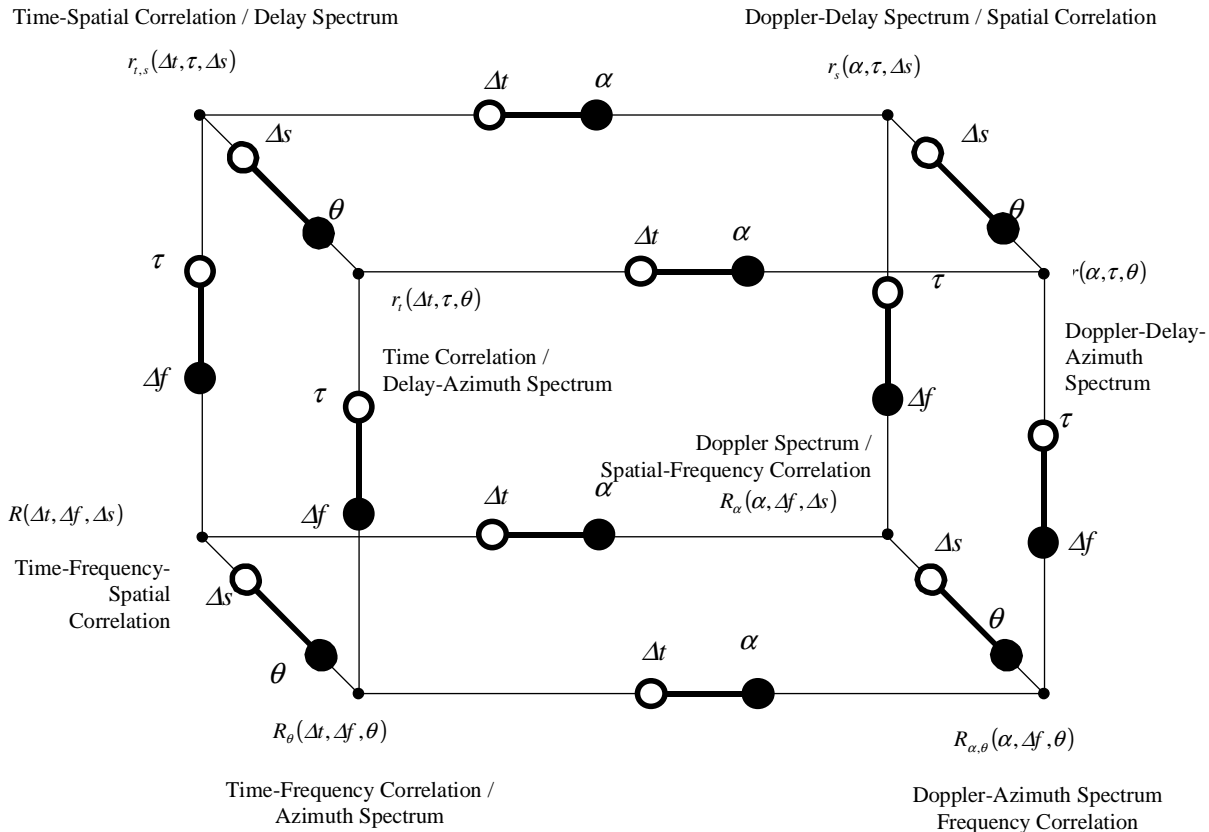


Fig. 3: WSSUS spectral and correlation relations.

7 Measurement examples

In the following, measurement results that are typical for an industrial environment are demonstrated. The measurement campaign took place in a car factory hall of the Daimler-Chrysler AG in Sindelfingen (Germany). Fig. 4, at first, shows the spatially averaged, magnitude-squared CIR sequence that was recorded with the Tx moving away from the Rx between two car assembly lines and subsequently driving around one of them and moving back toward the Rx. The sequence clearly shows the adequately changing delays. It also indicates that the LOS is lost during the way back. It can be expected that the channel parameters will change significantly at that instant since transmission will be based only on scattering and multiple reflection if LOS is obstructed. Fig. 5 shows more details from two cut-outs of the same impulse response at LOS conditions (left) and non-LOS conditions (right), respectively. From Fig. 6 the delay-

Doppler spectra at a LOS and a non-LOS location can be seen. The boundary projections in the 3-D pictures show the max-hold average delay spectrum and Doppler spectrum, respectively, that can be identified by the axis variables. In the non-LOS case an almost ideal classical Jakes Doppler spectrum occurs. Fig. 7a-c displays the short-time averaged delay-azimuth spectrum at two LOS-locations and at one non-LOS location. Here the boundary projections are the max-hold average azimuth spectrum and again the delay spectrum. It can be seen that the angular spread gradually decreases with increasing distance between Tx and Rx antenna during the LOS situation and suddenly increases when LOS is disappearing. The same characteristic is indicated in Fig. 8 where the r.m.s. angular spread and the r.m.s. delay spread are shown for the complete record length.

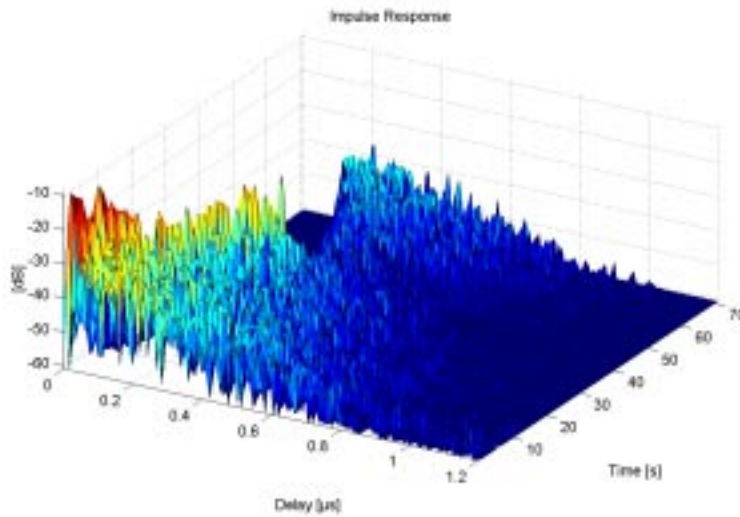


Fig. 4: Spatially averaged, log. magnitude squared impulse response (complete measurement drive).

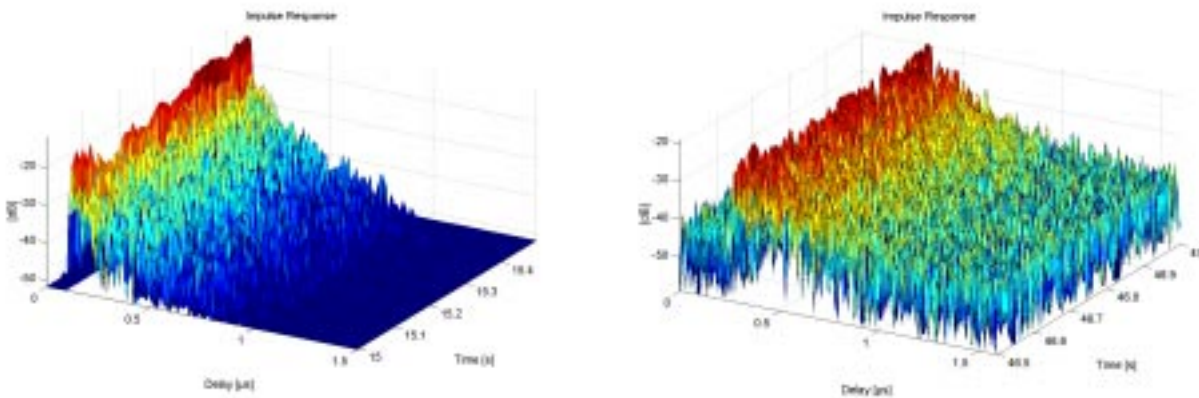


Fig. 5: Spatially averaged, log. magnitude squared impulse response: cut-out at 15 s (left) and at 47 s (right).

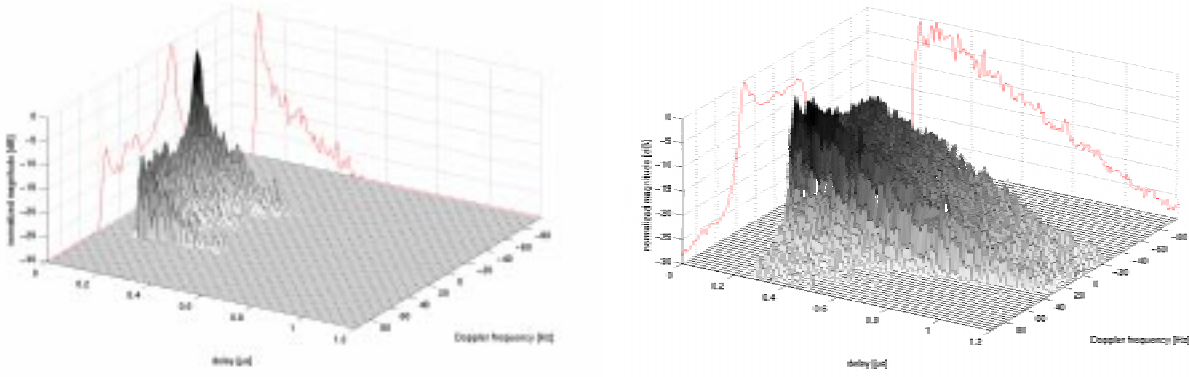


Fig. 6: Spatially averaged Delay-Doppler spectrum at 11 s (left) and at 60 s (right).

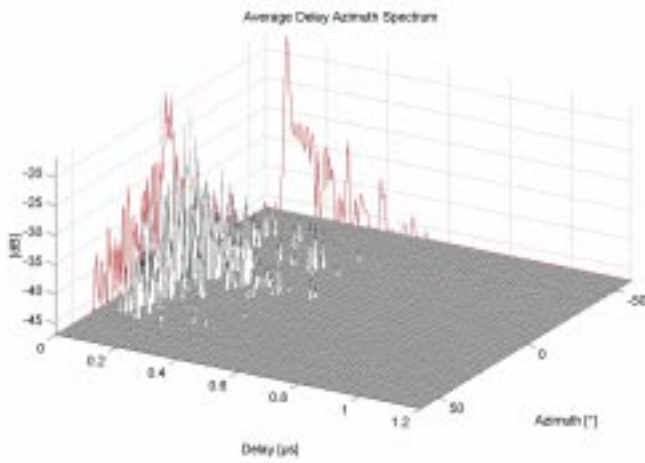


Fig. 7a: Local time averaged delay-azimuth spectrum at 7 s.

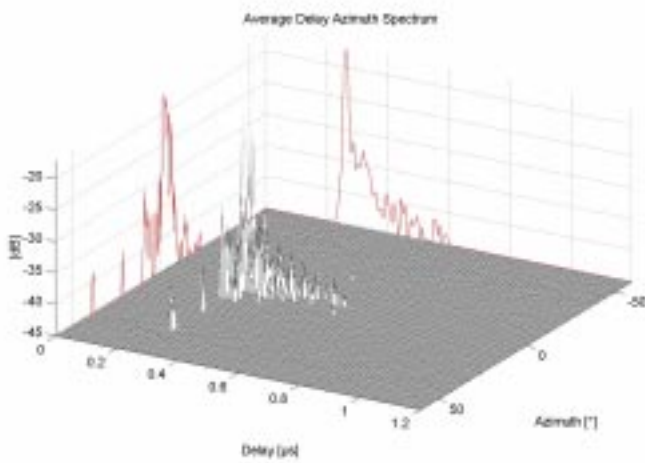


Fig. 7b: Local time averaged delay-azimuth spectrum at 38 s.

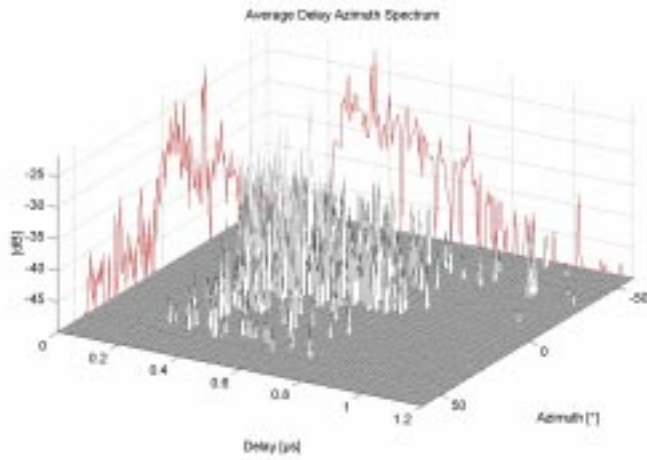


Fig. 7c: Local time averaged delay-azimuth spectrum at 55 s.

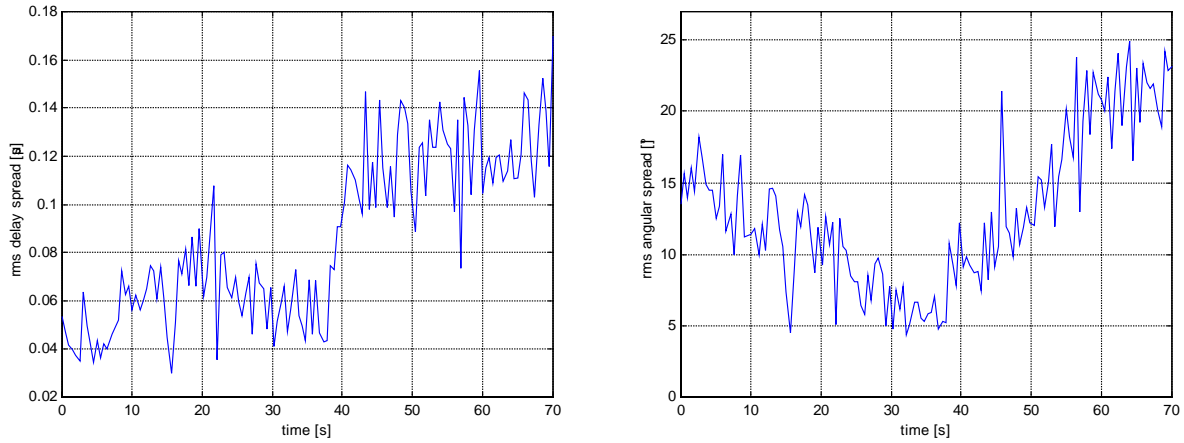


Fig. 8: r.m.s. delay spread (left) and r.m.s. angular spread (right) along the complete record.

8 Conclusions

A hardware-effective realization of a real-time vector channel sounder based on fast antenna multiplexing has been shown. That device allows full statistical analysis of the Doppler-delay-azimuth statistic of mobile radio channels. Further investigations will include elevation and polarization analysis as well. Also correlation of the delay-azimuth statistics between different frequency bands is of interest for investigation of uplink- and downlink-beamforming in frequency duplex systems. Estimation of parametric channel models and the usage of the measured channel responses for realistic link level simulation in different scenarios including dynamic changing situations are a further issue [15], [16].

Analysis of the radio channel under different model scenarios needs careful planning, extensive measurement campaigns and intensive analysis of the recorded data [18]. Effective software tools are required for that purpose.

Acknowledgements

This work is partly supported by the German Federal Ministry of Education, Science Research and Technology under the ATMmobil project line and partly by the DFG (Deutsche Forschungsgemeinschaft). The authors are grateful to MEDAV GmbH (<http://www.medav.de/>) for cooperation in development of the Vector Channel Sounder RUSK ATM and to the consortium of the EU project METAMORP for cooperation in channel sounder calibration and channel parameter definition.

References

- [1] A.J. Paulraj, C.B. Papadias, "Space-Time Processing for Wireless Communications," *IEEE Sig. Proc. Mag.*, vol.14, no.6, pp. 49-83, Nov. 1997
- [2] R.B. Ertel, P. Cardieri, K.W. Sowerby, T.S. Rappaport, J.H. Reed, "Overview of Spatial Channel Models for Antenna Array Communication Systems," *IEEE Personal Comm. Mag.* vol. 5, no. 1, pp. 10-22, Febr. 1998
- [3] U. Martin, "Spatio-Temporal Radio Channel Characteristics in Urban Macrocells," *IEE Proc. Radar, Sonar, Navig.*, vol. +145, no. 1, pp. 42-49, Febr. 1998
- [4] W. Kozek, "On the Transfer Function Calculus for Underspread LTV Channels," *IEEE Trans. SP*, vol. 45, no.1, Jan. 1997.
- [5] R.S. Thomä, H. Groppe, U. Trautwein, J. Sachs, "Statistics of Input Signals for Frequency Domain Identification of Weakly Nonlinear Systems in Communications," *IEEE Instr. and Measurement Technology Conf.*, Brussels, pp. 2-7, Juni 4-6, 1996
- [6] R.S. Thomä, D. Hampicke, A. Richter, G. Sommerkorn, A. Schneider, U. Trautwein, "Identification of Time-Variant Directional Mobile Radio Channels," *16th IEEE Instrumentation and Measurement Technology Conference, IMTC/99*, Venice, Italy, May 24-26, 1999, accepted for publication.
- [7] K. Schwarz, U. Martin, H.W. Schüßler, "Devices for Propagation Measurement in Mobile Radio Channels," *Proc. of the 4th IEEE Int. Symp. on Personal Indoor and Mobile Radio Communications, PIMRC'93*, Yokohama, Japan, pp. 387-391, Sept. 1993.
- [8] H. Krim, M. Viberg, "Two Decades of Array Signal Processing – the Parametric Approach," *IEEE Sig. Proc. Mag.*, vol.13, no.4, pp. 67-94, July 1996.
- [9] B.H. Fleury, D. Dahlhaus, R. Hedergott, M. Tschudin, "Wideband Angle of Arrival Estimation Using the SAGE Algorithm," *Proc. of the 4th IEEE Int. Symp. on Spread Spectrum Techniques and Applications, ISSSTA'96*, pp. 79-85, Mainz, Sept. 1996
- [10] M. Haardt, J.A. Nosssek, "Unitary ESPRIT: how to obtain increased estimation accuracy with reduced computational burden," *IEEE Trans. Signal Processing*, vol. 43, pp. 1232-1242, May 1995
- [11] M. Haardt, "Efficient One-, Two-, and Multidimensional High-Resolution Array Signal Processing," Shaker Verlag, Aachen, Germany, 1996, ISBN 3-8265-2220-6
- [12] K. Pensele, J.A. Nosssek, "Uplink and Downlink Calibration of an Antenna Array in a Mobile Communication System," *COST 259 Technical Document, TD(97)55*, Lisbon, Portugal, Sept. 1997
- [13] P. H. Lehne (Ed.), "Review of Existing Channel Sounder Measurement Setups and Applied Calibration Methods," Measurement, Testing and Calibration of Advanced Mobile Radio-Channel Equipment (METAMORP), Deliverable META/D-1/TR/D-1/1/b1, June 1998, <http://www.nt.tuwien.ac.at/mobile/projects/METAMORP/>
- [14] S.L. Marple, "Digital Spectral Analysis," Prentice Hall, 1987
- [15] U. Trautwein, K. Blau, D. Brückner, F. Herrmann, A. Richter, G. Sommerkorn, R.S. Thomä, "Radio Channel Measurement for Realistic Simulation of Adaptive Antenna Arrays," *The 2nd European Personal Mobile Communications Conference, EPMCC '97*, Bonn, Germany, pp. 491-498, Sep. 30 - Oct. 2, 1997.
- [16] U. Trautwein, G. Sommerkorn, R.S. Thomä, "A Simulation Study on Space-Time Equalization for Mobile Broadband Communication in an Industrial Indoor Environment," *IEEE Conf. Vehicular Technology, VTC Spring 1999*, Houston, Tx, accepted for publication.
- [17] U. Martin, "Statistical Mobile Radio Channel Simulator for Multiple-Antenna Reception," *IEICE 1996 International Symposium on Antennas and Propagation*, Chiba, Japan, pp. 217-220, Sept. 1996
- [18] U. Martin, J. Fuhl, I. Gaspard, M. Haardt, A. Kuchar, C. Math, A.F. Molisch, R.S. Thomä, "Model Scenarios for Intelligent Antennas in Cellular Mobile Communication Systems – Scanning the Literature." Submitted to *Wireless Personal Communications, Special Issue on Space Division Multiple Access*.

Identification of Time-Variant Directional Mobile Radio Channels

R.S. Thomä, D. Hampicke, A. Richter, G. Sommerkorn, A. Schneider, U. Trautwein

Key Word Index

Key Word	<i>page</i>
smart antennas	1
directional radio channel	1
direction of arrival (DOA)	2
Doppler shift	2
Doppler-azimuth-variant impulse response	2
time-space-variant frequency response	2
vector radio channel sounder	3
channel response vector snapshot (CRVS)	3
uniform linear array (ULA)	4
ESPRIT (Estimation of Signal Parameters via Rotational Invariance Techniques)	4
unitary ESPRIT	5
superresolution	5
signal subspace	5
spatial smoothing	6
joint delay-azimuth estimation	6
antenna beam patterns	6
antenna array calibration	6
wide-sense stationary uncorrelated scattering (WSSUS) channels	7
expected Doppler-delay-azimuth spectrum	7
delay-azimuth resolution	7
delay-azimuth spectrum	9